JOURNAL OF SPACECRAFT AND ROCKETS
Vol. 46, No. 4, July–August 2009

Hypersonic Low-Density Aerothermodynamics of Orion-Like Exploration Vehicle

R. Votta,* A. Schettino,† G. Ranuzzi,‡ and S. Borrelli§
Italian Aerospace Research Center—CIRA, 81043 Capua, Italy

DOI: 10.2514/1.42663

In the framework of Research Task Group 043 of the NATO Research and Technology Organization, an analysis of the capabilities in prediction of aerothermal loads acting on a crew exploration vehicle at the higher altitudes of its reentry trajectory has been performed. In particular, the focus of this investigation is to provide information where overlap between the continuum approach (i.e., computational fluid dynamics) and particle approach (i.e., direct simulation Monte Carlo) occurs and improves understanding of relevant physics in transitional regime. Computational fluid dynamics calculations with slip flow boundary conditions had shown good predicting capabilities of slip velocity, slip temperature, and pressure, but not the surface heat flux. The analysis of the contributions to the total surface heat flux had exhibited the lack of continuum model in evaluating the convective heat flux in the transitional zone of the Orion reentry trajectory and an underestimation of shock wave thickness.

Nomenclature

d	=	density, kg/m^3
Kn	=	Knudsen number, λ/L
L	=	reference length, m
M	=	Mach number
mcs	=	mean collision separation distance, m
N	=	number density, 1/m^3
P	=	pressure, Pa
Re	=	Reynolds number
s	=	curvilinear abscissa, m
T	=	temperature, K
X	=	molar fraction
λ	=	mean free path, m

Subscripts

D	=	diameter, m
n	=	normal component
r	=	rotationale
S	=	slip
t	=	translational
v	=	vibrational
W	=	wall
τ	=	tangential component
∞	=	freestream conditions

I. Introduction

THE main purpose of the present work is to study of predicting capabilities of aerothermal loads acting on a blunt body space reentry vehicle in transitional flow regime.

Received 9 December 2008; revision received 25 February 2009; accepted for publication 3 March 2009.

*Research Engineer, Aerothermodynamics and Space Propulsion Laboratory, Via Maiorise.
†Senior Research Engineer, Aerothermodynamics and Space Propulsion Laboratory, Via Maiorise.
‡Research Engineer, Aerothermodynamics and Space Propulsion Laboratory, Via Maiorise.
§Head of Aerothermodynamics and Space Propulsion Laboratory, Via Maiorise.

Moss et al. [1,2] analyzed the aerodynamic behavior of NASA's Orion crew exploration vehicle (CEV) capsule from hypersonic free molecular conditions to continuum conditions. In particular these investigations were focused on the assessment of computational tools that will be used to support the development of aerodynamic databases for future capsule fight environments. A direct simulation Monte Carlo (DSMC) method has been used to predict the transitional flow regime and a computational fluid dynamics (CFD) code for the continuum regime.

In the present work an aerothermal analysis on Orion capsule has been also conducted in transitional zone, in particular for the range of altitudes where both modelling (i.e. continuum by means of CFD and particle one by means of DSMC) could be used in order to compare the obtained results and to understand the physical reliability of each model; moreover, a sensitivity analysis with respect to the surface boundary conditions has been performed.

In addition, slip flow boundary conditions have been implemented in the CFD code in order to take into account effects of rarefaction in the continuum code. These kinds of conditions have already been tested as the hollow cylinder flare in hypersonic wind tunnel conditions [3] in prediction of local effects of rarefaction in shock wave boundary layer interaction phenomena. One of the main purposes of the present research activity is to verify the reliability of these kinds of boundary conditions for the evaluation of local aerothermal parameters also for a blunt body configuration in the transitional part of a classic reentry trajectory, where the effects of rarefactions has to be taken into account.

These investigations are also being treated by the scientific community in the framework of the RTO-RTG043 working group, and a brief description is reported.

The main purpose of the RTO-RTG043 working group is to identify and mitigate current inadequacies in present aerothermal prediction capabilities by advancing our understanding and modeling of the relevant physics and by incorporating these advancements in evolving aerothermal design tools. Different data are needed to this scope: assess what was learned in the past (gaps, uncertainties), assess measurement techniques, conduct experiments (improved measurement techniques), and conduct computational simulations of experiments.

In the framework of RTO-RTG043, six work topics are planned: nose and leading edges, shock interactions and control surfaces, chemical kinetics and radiation, boundary layer transitions, gas/surface interactions, and base and afterbody flows.

In this paper the nose and leading edges work topic will be presented and analyzed.

In this topic, six test cases have been proposed. The first is a numerical rebuilding of experimental test cases performed in

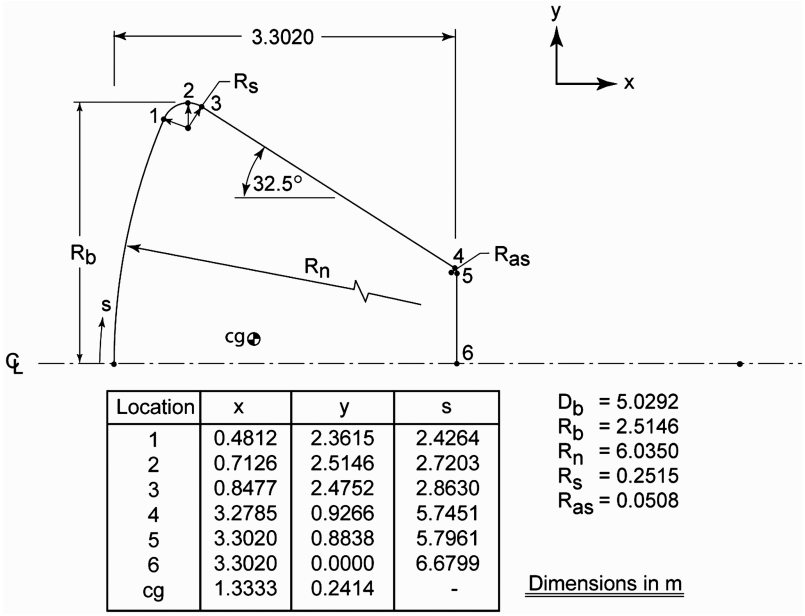

Location	x	y	s
1	0.4812	2.3615	2.4264
2	0.7126	2.5146	2.7203
3	0.8477	2.4752	2.8630
4	3.2785	0.9266	5.7451
5	3.3020	0.8838	5.7961
6	3.3020	0.0000	6.6799
cg	1.3333	0.2414	-

D_b = 5.0292
R_b = 2.5146
R_n = 6.0350
R_s = 0.2515
R_{as} = 0.0508

Dimensions in m

Fig. 1 Orion crew exploration vehicle, reference geometry.

different NASA ground facilities on the Mars science laboratory model to be used to validate CFD tools. The second is a numerical simulation for FIRE II flight conditions and then assess the current capabilities to predict heating along the forebody. Then, the Orion CEV test case is to be used to evaluate high-altitude aerothermodynamics of the Orion CEV. Another proposed test case concerns the 3-D interaction simulations in rarefied flows for tethered systems. Measurements and numerical simulations for leading edge heating with shock interactions is also proposed. The final planned test case is the coupled aerothermal simulation on the CIRA (Italian Aerospace Research Center) SCIROCCO plasma wind tunnel test case on sharp, hot structures.

As already underlined, CIRA is involved in the nose and leading edge work topic, referring to the evaluation of high-altitude aerothermodynamics of the Orion CEV.

The Orion CEV [4] is a spacecraft design currently under development by the U.S. space agency NASA, as announced by the NASA Constellation Program for exploring the moon, Mars, and beyond. The findings of the Exploration Systems Architecture Study recommended the use of an Apollo-like capsule. Some modifications have been done; CEV is much larger than Apollo, the mass is almost twice, and, like Apollo, it will be attached to a service module for life support and the propulsion system. The capsule will be launched by ARES I.

The Orion crew module will hold four to six crew members, compared with a maximum of three in the smaller Apollo. Different mission applications can be performed by CEV: a low-Earth-orbit version with a crew of six to the International Space Station (ISS), a lunar version that would carry a crew of four, and a Mars version that would carry a crew of six.

The heritage of Apollo's databases [1] has provided the design of CEV, of which the reference geometry is shown in Fig. 1.

The baseline flight conditions suggested in the framework of the nose and leading edges' activities for the CEV vehicle are representative of conditions that take place during the reentry trajectory from the ISS and corresponding to altitudes of 125, 115, 105, 95, 85, and 75 km.

The baseline assumptions are the following: fixed wall temperature, freestream velocity of 7.6 km/s for all altitudes, axis-symmetric geometry, and a zero angle of attack. In addition, a sensitivity analysis was performed with respect to the surface catalycity.

Freestream conditions as a function of altitude are listed in Table 1.

II. Numerical Approaches

A. Navier–Stokes Method

The continuum regime results have been obtained by using the CIRA CFD code H3NS developed at the Aerothermodynamics and Space Propulsion Laboratory [5]. The code solves full Reynolds-averaged Navier–Stokes equations, and considers the air flow in thermochemical nonequilibrium. The Park model with five species (O, N, NO, O_2, N_2) and 17 chemical reactions [6] is implemented, and the energy exchange between vibrational and translational temperature is based on Landau–Teller nonequilibrium equation, with average relaxation times taken from the Millikan–White [7] theory modified by Park [8]. The viscosity coefficient for the single species is computed by means of Yun and Mason collision integrals [9], whereas the conductivity coefficient uses Eucken's law. These coefficients for the gas mixture are calculated using semi-empirical Wilke formulas. Diffusion coefficients are obtained by Yun and Mason tabulated collision integrals [9].

From the numerical point of view, the code is based on a finite volume approach with a cell-centered formulation. The inviscid fluxes are computed by a flux difference splitting scheme [10] second-order approximation is obtained with an essentially non-oscillatory reconstruction of interface values. Time evolution is

Table 1 Freestream conditions as a function of altitude

Altitude, km	T_∞, K	N_∞, m^{-3}	d, kg/m^3	X_{O_2}	X_{N_2}	X_O	T_w, K	$Kn_{\infty,D}$
75	200	9.01E + 20	4.34E − 05	0.2372	0.7628	0.0000	1464	0.0003
85	181	1.65E + 20	7.96E − 06	0.2372	0.7628	0.0000	1184	0.0019
95	189	2.90E + 19	1.38E − 06	0.1972	0.7869	0.0159	951	0.01
105	211	4.98E + 18	2.30E − 07	0.1528	0.7819	0.0653	760	0.06
115	304	9.86E + 17	4.36E − 08	0.0979	0.7539	0.1484	618	0.32
125	433	3.06E + 17	1.31E − 08	0.0768	0.7117	0.2115	494	1.0

performed by an explicit multistage Runge–Kutta algorithm coupled with an implicit evaluation of the source terms.

To take into account the effects of rarefaction, slip boundary conditions have been employed. From the large number of available formulations of this kind of condition, the one proposed by Kogan [11] has been chosen. These boundary conditions have been obtained by matching the solution of the Boltzmann equation in the Knudsen layer to the solution of the macroscopic Navier–Stokes equations, thus yielding

$$V_s = 1.012\lambda\left(\frac{\partial V_\tau}{\partial n}\right)_w \tag{1}$$

$$T_s - T_w = 1.73\frac{\gamma}{\gamma-1}\frac{\sqrt{\pi}}{4}\lambda\left(\frac{\partial T}{\partial n}\right)_w \tag{2}$$

where V_S is the "slip velocity" and T_S the "slip temperature."

B. DSMC Method

The DSMC software used in this paper is the DS2V code of Bird [12–15], which is briefly described in the following paragraphs.

The DSMC method [14] considers the gas as made up of discrete particles that are represented by millions of simulated molecules; it relies on formulas from the kinetic theory of gases. Movement and evolution of each molecule in the simulated physical space is produced by collisions with other molecules and with the body under study, in both cases exchanging momentum and energy. Molecular collisions are simulated with the variable hard-sphere molecular model [14]. Energy exchange between kinetic and internal modes is controlled by the Larsen–Borgnakke statistical model [16]. All simulations are performed by using a five-species reacting air gas model while considering energy exchange between translation, rotational, and vibrational modes.

The computational domain, including the test body, is divided in cells; these are used only for sampling the macroscopic properties and for selecting the colliding molecules. Movement of each molecule from one cell to another is the product of the velocity (that is the resultant of the convective and thermal velocities) and a time step.

Macroscopic thermo-fluid-dynamic quantities of the flowfield (density, temperature, pressure, and so on) are computed in each cell as an average over the molecules.

DS2V uses transient subcells in which a transient background grid is built on a single cell and the collision routine, based on nearest-neighbor collisions, is applied. The resolution of the transient grid depends on the number of simulated molecules, and approximately one simulated molecule corresponds to one subcell.

DS2V provides in output, during the run, the ratio of the local mean separation between collision partners to the local mean free path (mcs/λ). This parameter is indicative of the quality of a run; it should be less than unity everywhere in the computational domain. Bird [12,13] suggests the value of 0.2 as a limit value.

The present applications rely on the fully accommodated Maxwell gas–surface interactions.

III. Results

A. Grid and Molecular Independence

A sketch of the 2-D CFD grid is shown in Fig. 2, where the shock fitting is clear.

The computational grid is composed of three blocks and 42,400 cells, with three grid levels. To check the grid convergence an analysis on different grid levels has been conducted. In particular, grid level 3 and level 2 (10,600 cells) results have been compared for the altitude of 95 km (see Table 1), for a fully catalytic wall conditions and a fixed wall temperature (i.e., $T_w = 951$ K).

The heat flux (variable more critical in variation with grid size) is computed by the two runs with different levels that are very close each other (Fig. 3), and so a grid independence has been verified.

The solution convergence has been obtained as the maximum and average residuals reach the stationary and, moreover, the surface heat flux (the most sensitive variable) does not change anymore during the iterations.

For what concerns the maximum value of the ratio of the local mean separation between collision partners to the local mean free path mcs/λ is 0.16 for the 95 km case and 0.69 for 85 km case.

B. Slip Flow Boundary Conditions Validation

To validate the Eqs. (1) and (2), a point of the Orion reentry trajectory has been chosen as a reference case to compare the results obtained by means of the continuum approach with slip flow correction and those obtained by means of the DSMC code. According to Moss [17], a general definition of the transitional regime is $10^{-3} < Kn_\infty < 50$, and so the altitude of 85 km (i.e., $Kn_\infty = 0.0019$), shown in the Table 1, has been selected to perform the comparison.

Figure 4 shows the good agreement between the slip velocity distribution at the wall predicted by CFD with the boundary conditions reported in Eq. (1) and DSMC result for a fully catalytic wall and a fixed wall temperature $T_w = 1184$ K. When the fixed wall temperature is 300 K (see Fig. 5) the good agreement between the two methodologies remains, and so the validity of Eq. (1) with the variation of wall temperature has been demonstrated.

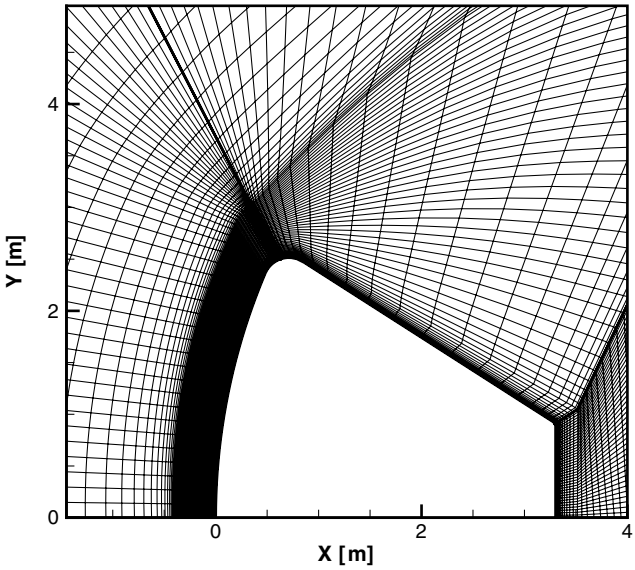

Fig. 2 CFD computational grid.

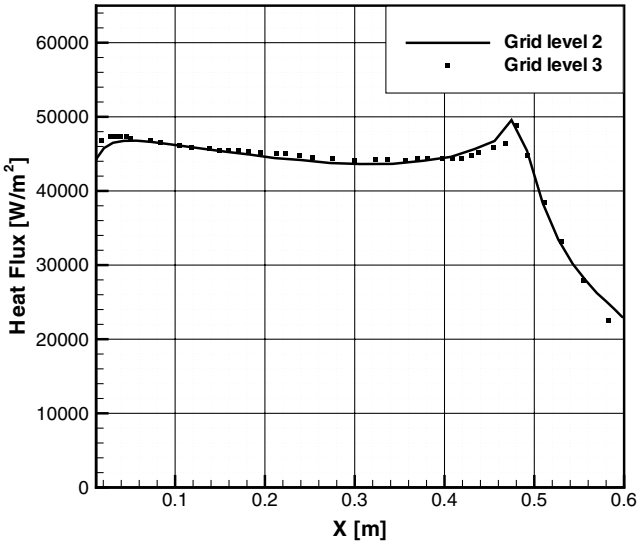

Fig. 3 Heat flux distribution where altitude = 95 km.

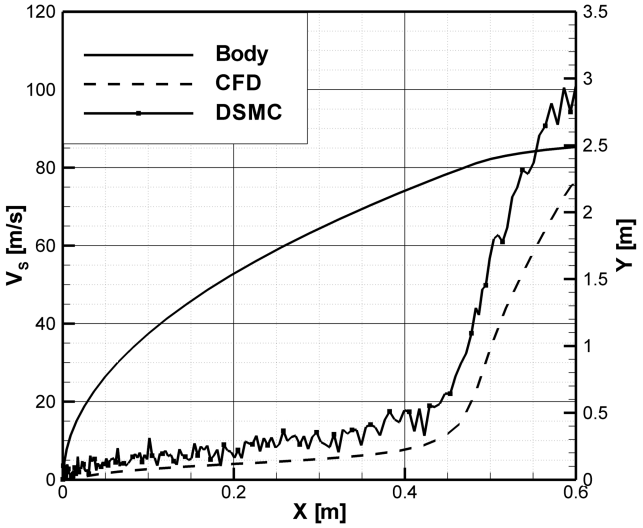

Fig. 4 Slip velocity distribution at altitude 85 km where $T_w = 1184$ K.

Also, the predicted slip temperature (see Fig. 6) obtained by means of the CFD code [Eq. (2)] is similar to the DSMC result. In particular, the slip temperature calculated using the CFD code is slightly higher with respect to the temperature computed by the particle code. This discrepancy is caused by the different modelling of temperature at the wall. In fact, in the CFD code, the translational and rotational temperatures are assumed in equilibrium, being only the vibrational temperatures considered in nonequilibrium, whereas a three-temperature gas model is implemented in DSMC code (rotational temperature T_r, translational temperature T_t, vibrational temperature T_v). Also, for calculation of the slip temperature Eq. (2) implemented in the CFD code has shown a good prediction as the fixed wall temperature varies (see Fig. 7).

C. Results

The focus of the present investigation is mainly on the 85 and 95 km cases. For these two trajectory points, both CFD and DSMC computations have been performed, including the sensitivity analysis with respect to some boundary conditions.

Figure 8 shows the pressure isolines for the altitude of 85 km and a fully catalytic wall condition. The flowfield calculated by the DSMC tool is compared with the flowfield calculated by CFD code (no significant difference is visible in the flowfields computed with and without slip flow boundary conditions), whereas Fig. 9 exhibits the pressure profiles along the stagnation line for all the analyzed methodologies. It can be clearly seen that the shock wave thickness

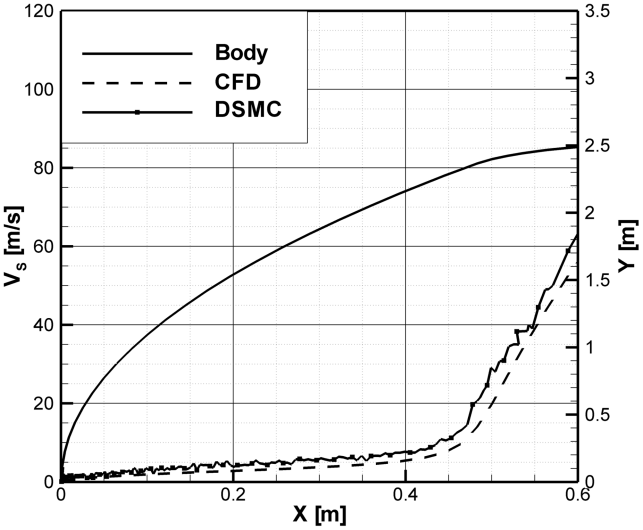

Fig. 5 Slip velocity distribution at altitude 85 km where $T_w = 300$ K.

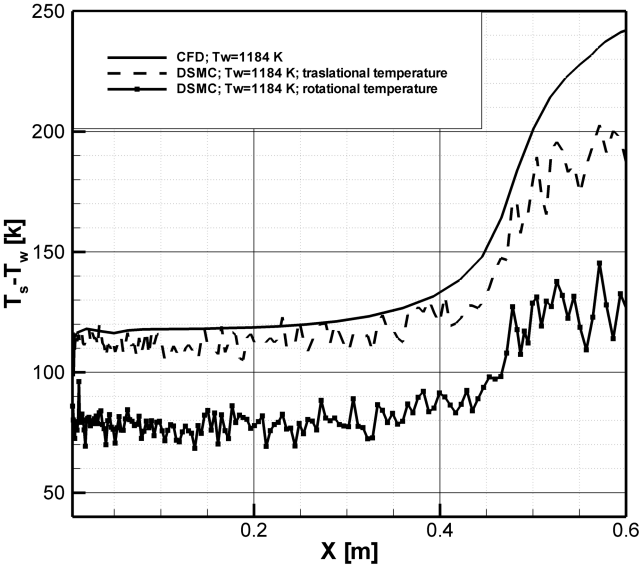

Fig. 6 Slip temperature distribution at altitude 85 km where $T_w = 1184$ K.

computed by the particle code is larger with respect to the Navier–Stokes codes; this value, generally expressed as a multiple of the upstream mean free path [14], is well predicted by the DSMC code for all the analyzed cases.

At 85 km of altitude, a fully catalytic wall, and $T_w = 1184$ K, the wall pressures computed by all methodologies (DSMC, CFD, and CFD with slip conditions) are very close each other (see Fig. 10).

The global drag coefficient is very similar among all the performed calculations (about 1.703) being the value of pressure very close to zero where it varies with the used methodology. It has been verified that the catalysis and the temperature at the wall does not influence the pressure profile at the wall.

Also at 95 km, in the forebody region and after the shock wave, all the used methodologies show a similar behavior in prediction of wall pressure (see Fig. 11). Instead (Fig. 12) some slight differences can be seen in the expansion zone (after the shoulder), where the flow is more rarefied (the local Knudsen number based on the boundary layer thickness is about 10^{-1}); in this zone the slip flow correction brings the CFD result to be closer to the DSMC result. Therefore, the drag predicted by CFD and DSMC simulations is very similar, and greater differences are expected at higher altitudes. As expected, the wall catalysis does not influence the wall pressure profiles.

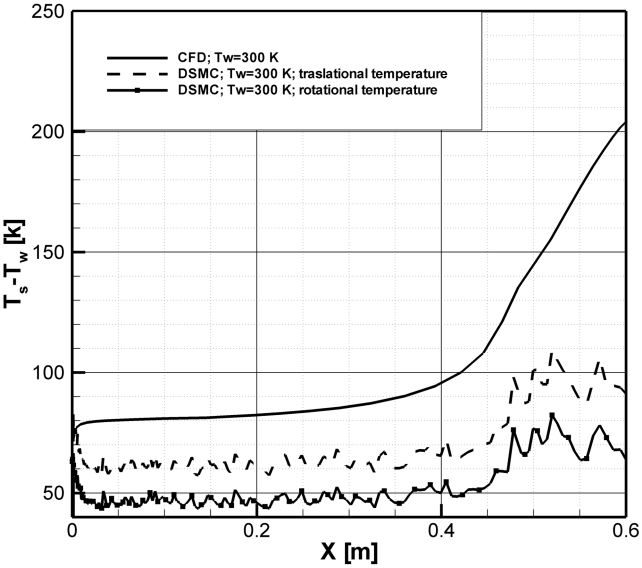

Fig. 7 Slip temperature distribution at altitude 85 km where $T_w = 300$ K.

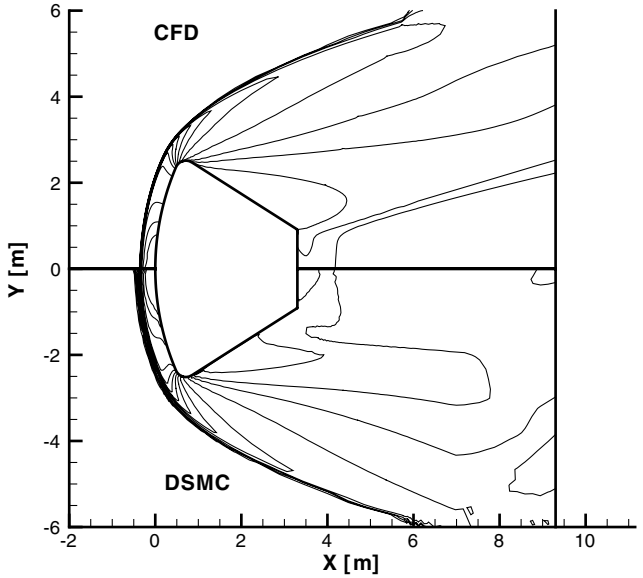

Fig. 8 Pressure isolines at altitude 85 km with a fully catalytic wall where $T_w = 1184$ K.

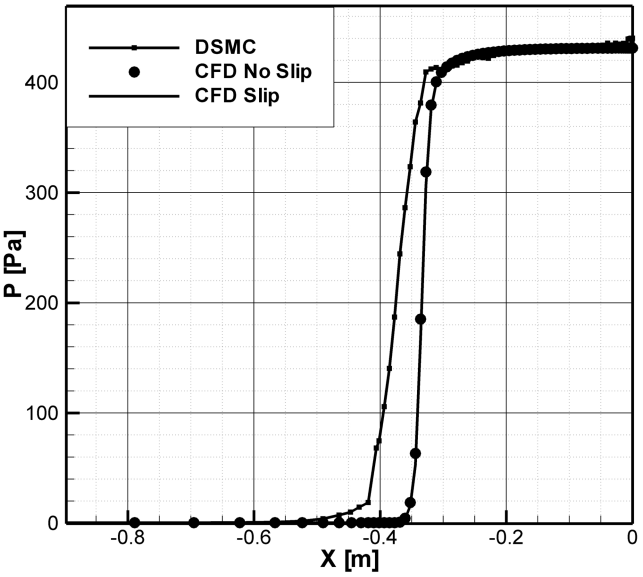

Fig. 9 Pressure profiles along the stagnation line at altitude 85 km with a fully catalytic wall where $T_w = 1184$ K.

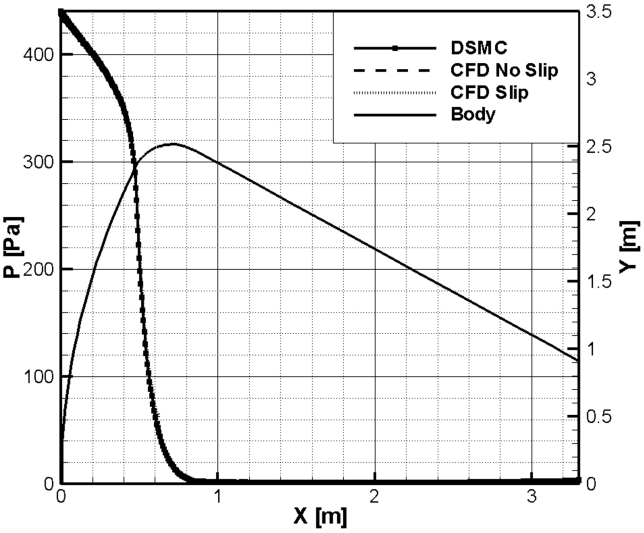

Fig. 10 Pressure profile at altitude 85 km with a fully catalytic wall where $T_w = 1184$ K.

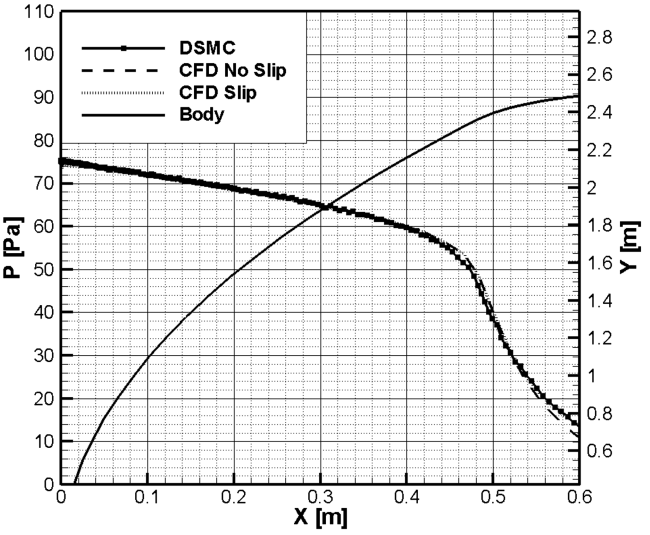

Fig. 11 Pressure profile at altitude 95 km with a fully catalytic wall where $T_w = 951$ K.

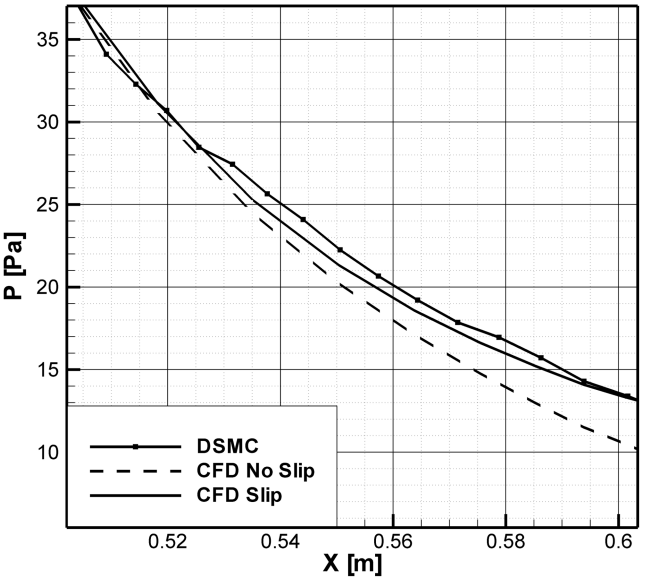

Fig. 12 Pressure profile at altitude 95 km with a fully catalytic wall where $T_w = 951$ K- zoom.

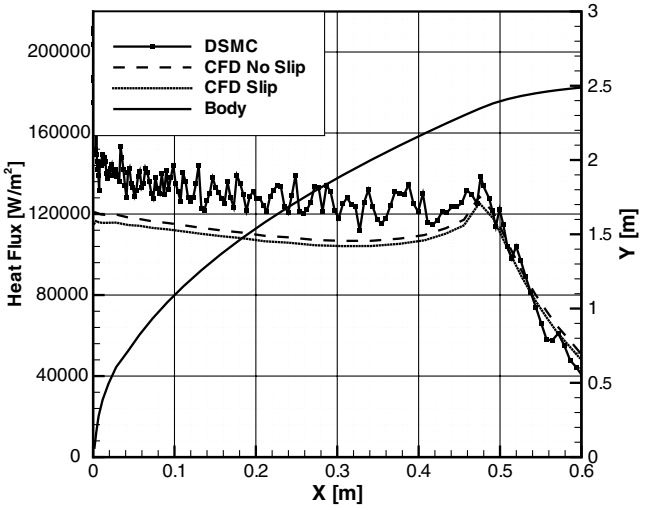

Fig. 13 Heat flux distribution at altitude 85 km with a fully catalytic wall where $T_w = 1184$ K.

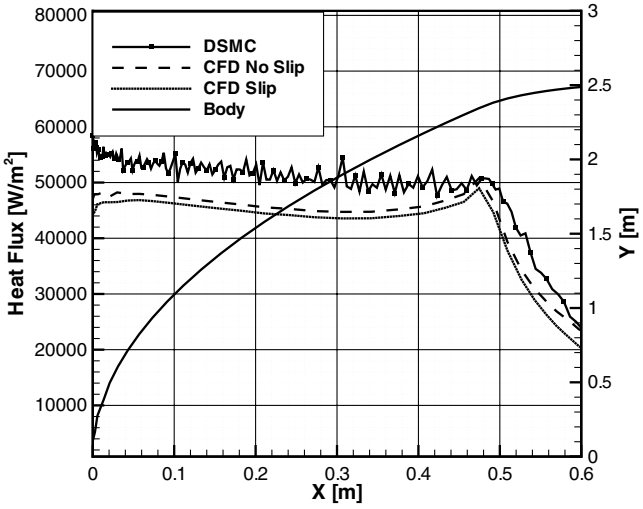

Fig. 14 Heat flux distribution at altitude 95 km with a fully catalytic wall where $T_w = 951$ K.

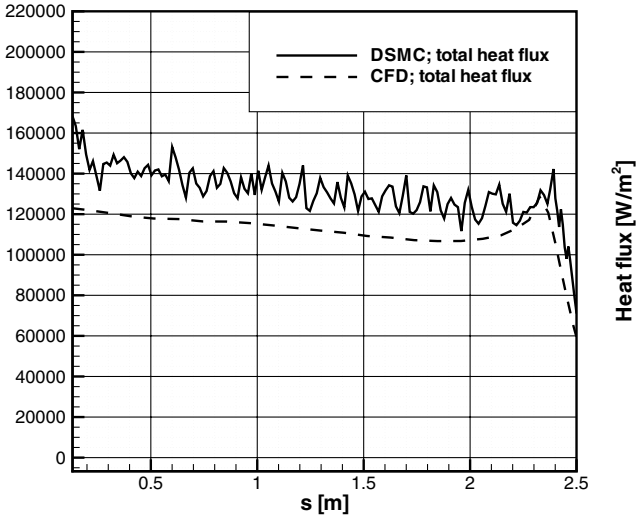

Fig. 15 Total heat flux distribution at altitude 85 km with a fully catalytic wall.

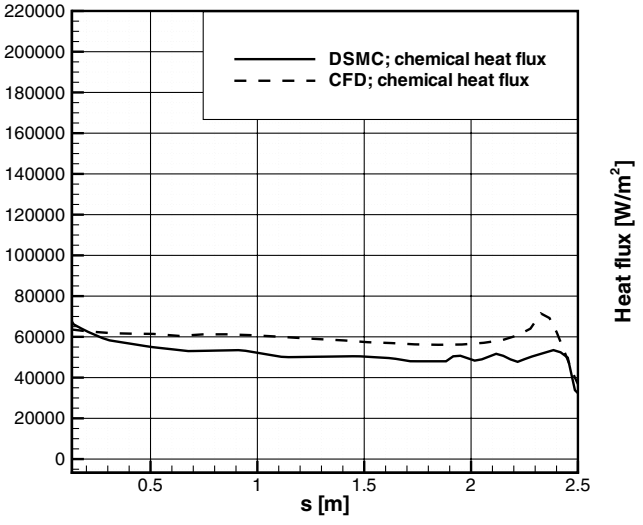

Fig. 16 Chemical heat flux distribution at altitude 85 km with a fully catalytic wall and chemical heat flux.

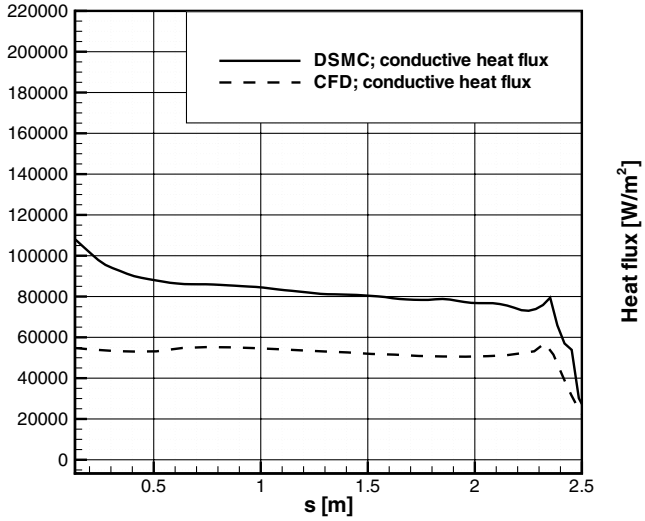

Fig. 17 Conductive heat flux distribution at altitude 85 km with a fully catalytic wall.

Figures 13 and 14 show, for the two trajectory points, the surface heat flux calculated by the DSMC tool and CFD tools (with and without slip flow boundary conditions). For both of the altitudes, the DSMC result is about 10% higher with respect to continuum results.

As expected, the heating reaches the maximum value in the stagnation region, and in the shoulder region where the strong expansion occurs a second peak is predicted by both CFD calculations but not by DSMC. It must be noted that the effect of the slip conditions in the CFD computations is very small; moreover, if one computes the heat flux by means of the classical Fourier formula, a decrease of heat flux is predicted by the "slip" case. Definitely, the slip flow correction gives good results in prediction of wall parameters such as slip velocity, temperature, and pressure but not in surface heat flux calculation.

An evaluation of the single contributions to the global heat flux is shown in Figs. 15–17, for 85 km of altitude and fully catalytic conditions. In particular, it can be seen that the chemical contribution to the heat flux calculated by the CFD is very close to that of the DSMC (see Fig. 16), whereas the conductive heat flux is lower (see Fig. 17). This difference on global heat flux is confirmed from the noncatalytic wall case showed in Fig. 18. It is interesting to note that in the noncatalytic case the percentage difference between CFD and DSMC results increases from about 10 to 60%, but the absolute value of this difference is the same as for fully catalytic wall; this confirms

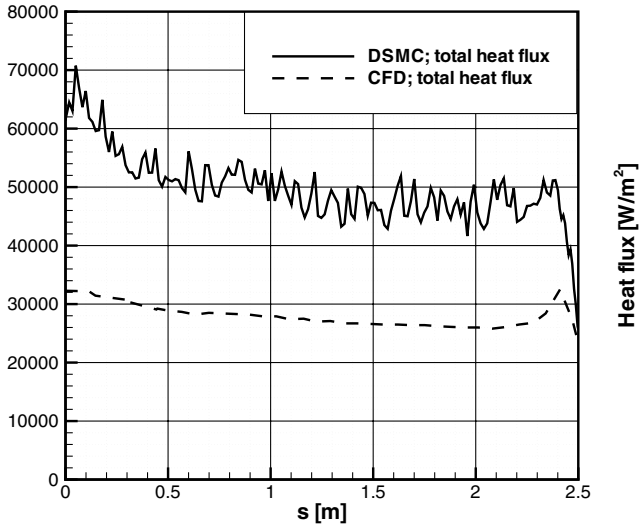

Fig. 18 Heat flux distribution at altitude 85 km with a noncatalytic wall.

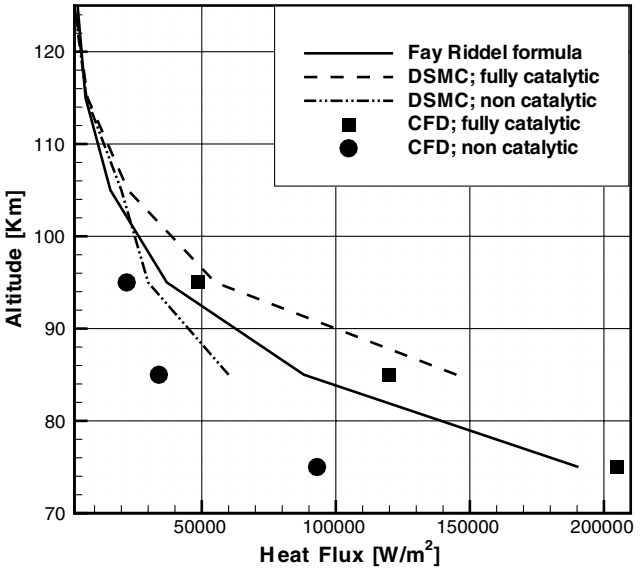

Fig. 19 Heat flux at the stagnation point vs altitude.

that the discrepancy is not due to the chemical part of the heat flux, but from the conductive part. The same considerations apply to the altitude 95 km case.

For the higher altitude points (i.e., 105, 115, and 125 km) of Table 1, continuum modelling is no longer applicable; therefore they have been computed only by means of the DSMC code. The 75 km case instead has been computed only by means of the CFD code, because the DSMC tool should need too much RAM Memory. Then, Fig. 19 summarizes the heat flux of the stagnation point for all the considered cases computed by the correct methodology for each altitude. As a reference, the Fay–Riddel formula, typically used for preliminary design of the thermal protection system (TPS), has been plotted. In the zone where both modelling could be applied (i.e., 85 and 95 km), DSMC values should be used, because CFD and the approximate formula underestimate the heat flux and, therefore, a correct prediction of rarefaction effects is needed.

IV. Conclusions

In the framework of the RTO-RTG043 working group the axis-symmetric aerothermodynamics of the Orion CEV in the transitional part of the reentry trajectory has been presented.

To this aim, the analysis has been mainly conducted on the altitudes 85 and 95 km, corresponding to a value of freestream Knudsen numbers 0.0019 and 0.01, respectively. Two theoretical approaches have been used: a particle approach (DSMC) and a continuum approach (CFD with and without slip flow boundary conditions).

Shock wave thickness calculated by DSMC code is larger with respect to CFD and in agreement with theoretical considerations for all the analyzed cases. All methodologies show a good match in prediction of the wall pressure in the forebody region, although some discrepancies appear in the expansion and base regions and increase with rarefaction of the gas (altitude). The global aerodynamic forces are not affected by the used methodology, being the differences located in a region where the pressure is much lower with respect to the forebody region.

The surface heat flux calculated by the DSMC code is about 10% higher than that of the CFD for the fully catalytic wall assumption, whereas this difference raises to about 60% in the case of a noncatalytic wall, because the discrepancy is mainly due to the conductive heat flux. Slip flow boundary conditions were implemented to take into account the effects of rarefaction of gas in the CFD code, and show good results in prediction of slip velocity, slip temperature, and pressure but not in the evaluation of the heat flux, as the higher value of the wall temperature causes an underestimation. Therefore, in general, the DSMC should be preferred with respect to CFD in the prediction of heat fluxes.

References

[1] Moss, J. N., Boyles, K. A., and Greene, F. A., "Blunt Body Aerodynamics for Hypersonic Low Density Flows," *Proceedings of 25th Symposium on Rarefied Gas Dynamics*, edited by Ivanov, M. S. and Rebrov, A. K., Vol. 1, Siberian Branch of the Russian Academy of Sciences, Saint-Petersburg, Russia, 2006, pp. 753–758.

[2] Moss, J. N., Boyles, K. A., and Greene, F. A., "Orion Aerodynamics for Hypersonic Free Molecular to Continuum Conditions," *14th AIAA International Space Planes and Hypersonic Systems and Technologies Conference*, AIAA Paper 2006-8081, Nov. 2006.

[3] Votta, R., Ranuzzi, G., Di Clemente, M., Schettino, A., and Marini, M., "Evaluation of Local Effects of Transitional Knudsen Number on Shock Wave Boundary Layer Interactions," *39th AIAA Thermophysics Conference*, AIAA Paper 2007-4545, June 2007.

[4] Lee, D. B., "Apollo Experience Report Aerothermodynamics Evaluation," NASA TN D-6843, June 1972.

[5] Ranuzzi, G., and Borreca, S., "CLAE Project. H3NS: Code Development Verification and Validation," CIRA CF-06-1017, 2006.

[6] Park, C., "A Review of Reaction Rates in High Temperature Air," AIAA Paper 89-1740, June 1989.

[7] Millikan, R. C., and White, D. R., "Systematic of Vibrational Relaxation," *The Journal of Chemical Physics*, Vol. 39, No. 12, 1963, pp. 3209–3213.

[8] Park, C., and Lee, S. H., "Validation of Multi-Temperature Nozzle Flow Code NOZNT," AIAA Paper 93-2862, 1993.

[9] Yun, K. S., and Mason, E. A., "Collision Integrals for the Transport Properties of Dissociating Air at High Temperatures," *The Physics of Fluids*, Vol. 5, No. 4, 1962, pp. 380–386.doi:10.1063/1.1706629

[10] Borrelli, S., and Pandolfi, M., "An Upwind Formulation for the Numerical Prediction of Non Equilibrium Hypersonic Flows," *12th International Conference on Numerical Methods in Fluid Dynamics*, Springer–Verlag, Berlin, 1990, pp. 416–420.

[11] Kogan, N. M., *Rarefied Gas Dynamics*, Plenum, New York, 1969.

[12] Bird, G. A., "Visual DSMC Program for Two-Dimensional Flows," *The DS2V Program User's Guide*, Ver. 2.1, URL: http://gab.com.au [retrieved Oct. 2006].

[13] Bird, G. A., "Visual DSMC Program for Three-Dimensional and Axially Symmetric Flows," *The DS2V Program User's Guide*, Ver. 2.1, URL: http://gab.com.au [retrieved Oct. 2006].

[14] Bird, G. A., *Molecular Gas Dynamics and the Direct Simulation of Gas Flows*, Clarendon, Oxford, 1994.

[15] Bird, G. A., "The DS2V/3V Program Suite for DSMC Calculations," *Rarefied Gas Dynamics, 24th International Symposium*, Vol. 762, edited by M. Capitelli, American Inst. Of Physics, NY, Feb. 1995, pp. 541–546.

[16] Borgnakke, C., and Larsen, P. S., "Statistical Collision Model for Monte Carlo Simulation of Polyatomic Gas Mixture," *Journal of Computational Physics*, Vol. 18, No. 4, 1975, pp. 405–420. doi:10.1016/0021-9991(75)90094-7

[17] Moss, J. N., "Rarefied Flows of Planetary Entry Capsules," *Proceedings of AGARD-R-808*, edited by AGARD, Von Kàrmàn Institute for Fluid Dynamics, Rhode-Saint-Genèse, Belgium, May 1997, pp. 95–129.

G. Palmer
Associate Editor